UCRL-16777

University of California

Ernest O. Lawrence Radiation Laboratory

FIELD ION MICROSCOPE STUDIES OF INTERFACES

TWO-WEEK LOAN COPY

This is a Library Circulating Copy which may be borrowed for two weeks. For a personal retention copy, call Tech. Info. Division, Ext. 5545

Berkeley, California

DISCLAIMER

This document was prepared as an account of work sponsored by the United States Government. While this document is believed to contain correct information, neither the United States Government nor any agency thereof, nor the Regents of the University of California, nor any of their employees, makes any warranty, express or implied, or assumes any legal responsibility for the accuracy, completeness, or usefulness of any information, apparatus, product, or process disclosed, or represents that its use would not infringe privately owned rights. Reference herein to any specific commercial product, process, or service by its trade name, trademark, manufacturer, or otherwise, does not necessarily constitute or imply its endorsement, recommendation, or favoring by the United States Government or any agency thereof, or the Regents of the University of California. The views and opinions of authors expressed herein do not necessarily state or reflect those of the United States Government or any agency thereof or the Regents of the University of California.

UCRL-16777

UNIVERSITY OF CALIFORNIA

Lawrence Radiation Laboratory
Berkeley, California

AEC Contract No. W-7405-eng-48

FIELD ION MICROSCOPE STUDIES OF INTERFACES

S. Ranganathan

(March 1966)

FIELD ION MICROSCOPE STUDIES OF INTERFACES

S. Ranganathan

Inorganic Materials Research Division
Lawrence Radiation Laboratory,
Berkeley, California

1. INTRODUCTION

Interfaces are of wide and varied occurrence. The boundary between two crystals forms just one type. The crystals themselves can differ in orientation, structure and composition. All three kinds of interfaces have been studied with the field ion microscope. However extensive studies have been confined to boundaries separating crystals differing only in orientation. The primary problem in this field has been to evolve a model for the atomic configuration at high angle grain boundaries. These attempts have met with some success. Other properties of grain boundaries are of interest: the scope for field ion microscope studies seems to be limited however. The article concludes with observations of boundaries separating crystals differing in structure and composition.

2. INCIDENCE OF GRAIN BOUNDARIES

In the transverse cross section ($\sim 10^{-4} cm^2$) of a wire of 0.1 mm diameter, there are 10,000 grains for a grain size of 1μ and thrice as many boundaries. The area imaged in the field ion microscope is of the order of $10^{-10} cm^2$. Hence the chances of imaging a grain boundary are expected to be low. In practice the chances are considerably improved as one samples a volume by the process of field evaporation. Also heating the tip in situ sometimes produces a migration of grain boundaries into the field of view. Simultaneous heating and deformation of the wire prior to preparation of the specimen, a suggestion due to McLean, led to a small grain size and

appreciably improved the chances of finding a grain boundary in the field of view. Certain recrystallization treatments appear to be critical: tungsten wire heated to 1000°C, and molybdenum wire heated to 700°C were particularly profitable materials to work with.

Brock[1] carried out a pioneering study of grain boundaries with the field emission microscope and followed a suggestion due to Müller to increase the incidence of grain boundaries. The tungsten specimen was thinned, bent and then a tip was sharpened of the bend. The tip was then annealed at 2400°K. It was believed that the prior deformation induces recrystallization and causes a number of grain boundaries to appear in the field of view. In a report, Müller has claimed that this method led to the appearance of grain boundaries in 90% of the tips so treated. In an early study of grain boundaries with the field ion microscope, Wolf[2] has made use of this technique. No extensive use of this method has been reported. A major drawback is that the tips will have large radius after annealing and the loss of resolution at large radii is especially serious when liquid nitrogen is used for cooling.

3. GRAIN BOUNDARY ANALYSIS

An arbitrary grain boundary has five degrees of freedom. Three are needed to define the misorientation between the two crystals. These three degrees of freedom can be given as an angular misorientation around an axis. If it is assumed that the field ion micrograph is a stereographic projection, standard crystallographic methods can be employed to determine the axis-angle pair. The first such determination with the field ion micrograph was made by Ralph and Brandon.[3] A great circle is drawn through two poles with the same indices, one in each crystal. The mid-point of the arc between the two poles is linked to the pole of the great circle by another great circle.

It is clear that the axis of misorientation lies on the second great circle. The intersection of this great circle with another similarly derived gives the axis of misorientation. Ralph and Brandon used any two poles. It seems preferable to operate with the cube poles arrived at after giving weight to the determination of the three poles (Fig. 1a). This graphical analysis has an accuracy of ±2° and the assumption of a stereographic projection aggravates the inaccuracy. Fortunately the b.c.c. metals exhibit a strong wire texture; the misorientations are usually around [110] and this pole is in the center of the micrograph. Hence greater confidence can be attached to these determinations than would seem possible at first sight.

Two degrees of freedom are required to specify the orientation of the boundary plane. Once again simple geometrical relations can be used. (See, for example, Hren[4].) Figure 1b illustrates the situation. The inclination of the pole of the plane to the axis of the wire is equal to $90° - \tan^{-1} \frac{\gamma \sin \alpha}{(N-n)h}$, where γ is the radius of the tip, α is the angle at which the pole (intersection of the boundary with the surface in a zone containing the axis of the wire) appears on one micrograph and N the number of planes of step height, h, required to be removed so that the point of intersection reached the center of the micrograph and n, the number of rings counted from the center to the pole (intersection). This expression is different from the one used by Hren[4]. One could distinguish three types of boundaries on the basis of this equation and the relation between N and n. (1) $N = \infty$ i.e. the intersection of the boundary with the surface does not seem to move with field evaporation. Most boundaries are of this type. This appears to indicate that this is a stable configuration attained by grain boundaries because of the large kinematical freedom they enjoy in the small volume of the tip. (2) $N = n$. The pole of the boundary is the same as the

axis of the wire. This is of unusual occurrence and is in line with the expectation that such transverse boundaries will tend to "flash" the tip. (3) $N \neq n$. The boundary is inclined to the axis of the wire and its intersection with the surface is seen to move on field evaporation. All three cases and their appearance on a stereographic projection are illustrated in Fig. 1C.

4. STRUCTURE OF LOW ANGLE BOUNDARIES

The observation of etch pits at the emergence of dislocations and direct electron microscopic observations of dislocation arrays have fully substantiated the dislocation model of Burgers and Bragg for low angle boundaries. The review by Amelinckx and Dekeyser[5] gives an excellent and rigorous treatment of this model. A symmetrical tilt boundary consists of a row of parallel edge dislocations at appropriate distances to give the required misorientation. A twist boundary consists of a crossed grid of screw dislocation. More complicated arrays are required when there is a departure from these strict conditions. Field ion microscope observations are of a confirmatory nature. They are considered below as they bring out interesting details with regard to contrast in field ion micrographs.

If there are to be five dislocations in the field of view, the dislocations will be about 60Å apart. This distance of separation will correspond in the case of a simple tilt boundary to a misorientation of 3°. The grain boundary in iridium shown in Fig. 2 has a misorientation of 2° around [111]. The plane of the boundary was inclined to the axis of the wire and on field evaporation, the boundary intersected the surface at a different place. The asymmetry of the tip made an accurate determination of the plane of the boundary impossible. The streaks occur on $(01\bar{1})$

planes in f.c.c. metals. The intersection of the boundary is parallel to the streaks showing that their poles occur in the same zone. This fact and the movement of the boundary intersection pointed to (120) as the boundary plane. Hence the boundary has twist character and must have screw dislocations making up the array.

The dislocation structure seen in Fig. 2 has the appearance of a "classical" screw dislocation. If the boundary plane is (111) and if the axis of misorientation is [111], the model for the boundary consists of a hexagonal grid of dislocations having Burgers vectors $\frac{a}{2}[1\bar{1}0]$, $\frac{a}{2}[\bar{1}01]$, and $\frac{a}{2}[01\bar{1}]$. When the orientation of the boundary plane is changed, e.g., to (120), there is only a change in the mesh shape and the pattern becomes such that its projection along the [111] on a (111) plane produces the same hexagonal net. The dislocation seen at the boundary must form part of such a grid. However the Burgers vectors of the dislocation must be of the type $\frac{a}{2}[110]$ or $\frac{a}{2}[101]$ or $\frac{a}{2}[011]$. $\frac{a}{2}[1\bar{1}0]$, $\frac{a}{2}[\bar{1}01]$ and $\frac{a}{2}[01\bar{1}]$ all lie on the (111) plane and hence will not give rise to a spiral based on (111) planes. The dislocation is thus probably a stranger dislocation in the network.

Interlocked and interleaved spirals have been observed at low angle boundaries in tungsten and molybdenum. They are not easily analyzed into the component dislocations.

5. STRUCTURE OF TWIN BOUNDARIES

A twin boundary is said to be coherent when the twin plane and the composition plane coincide [(111) in f.c.c. and (112) in b.c.c.]; and noncoherent when this condition is not fulfilled. In-coherent twins the atoms in the composition plane are in correct position with respect to

both lattices. The twin boundary energy is correspondingly low.

Müller[6] has presented an example of what appears to represent a small angle twin boundary with (100) as the boundary plane. A mirror image is seen across this plane. The use of the phrase "small angle twin" is not clear in this context. He has also observed a twin boundary in steel with (121) as the boundary plane.[7] This is presumably a coherent twin and the atomic matching is excellent.

A few noncoherent annealing twins have been observed in tungsten. A particularly interesting case showing exceptionally good atomic matching has been analyzed in detail by Hren.[4] Figure 3 shows a similar twin in tungsten. The misorientation 180° rotation around [112] is seen very clearly. The plane of the boundary is a few degrees from $(\bar{1}13)_A$ and $(2\bar{2}3)_B$. The plane is of moderately high atomic density and will have one in three atoms in coincidence sites. Because of the deviations in the orientation of the boundary plane, several ledges were observed in the boundary (Fig. 3a). The structure of such ledges is discussed in a later section.

Twinning is a mode of deformation and is especially favored at low temperatures and high strain rates in the case of b.c.c. metals (Hall[8]). In three instances deformation twinning of the tips was observed. Figures 4 and 5 were obtained before and after the twinning transformation. The poles [110] and [112] remain in the same position as a twin can be related by a 70.5° rotation around [110] and a 180° rotation around [112]. It will also be noted that the zone decoration line has rotated through 70°. The tip was originally hemispherical and has become ellipsoidal as a result of twinning. There is considerable stress relief and the tilt in the surface could have led to the observed streaking.

In another case twinning occurred as the voltage was raised to the value necessary for imaging. The boundary region appeared as a chasm at first and gradually this closed up. A cavity can still be seen in Fig. 6. The twin relationship is obvious. The spiral effect implies that a dislocation structure has been added to the boundary. The spiral is similar to the one observed at the low angle boundary in iridium. The continuity of the spiral is interrupted at the ninth plane where a second dislocation might be intersecting the surface. The twin has a noncoherent interface and the plane of the boundary is very near $\{112\}_A$ and $\{110\}_B$. Both are close-packed planes in the b.c.c. lattice and this explains the excellent atomic matching across the boundary. The dislocation observed near the central (110) pole will explain the slight deviation in the plane of the boundary from the close-packed planes. In this case the orientation relationship is exact and hence there is no superposed small angle boundary.

With field evaporation, the spiral remained in the same place thus showing that the dislocation was running in the (110) direction. Similar spirals arising through evaporation have been observed on a macroscopic scale by Votava and Berghezan.[9] They ascribed the spirals to twinning dislocations. It is difficult to see how a single twinning dislocation can give rise to a simple spiral. The suggestion of Ryan and Suiter[10] that these structures result from slip dislocation adsorbed at the boundary is attractive. However even in this case because the crystals are rotated with respect to each other the continuation of the atomic planes across the boundary is surprising.

6. STRUCTURE OF SPECIAL AND RANDOM BOUNDARIES

6.1 Theory

As a result of the field ion microscopic observations of the structure of grain boundaries, a new model for the atomic configuration at high angle boundaries has been evolved by Brandon, Ralph, Ranganathan and Wald.[11] The coincidence site lattice relationships forming the basis of this theory were worked out by the author.[12]

Rotational symmetry operations on a lattice bring it into complete self-coincidence. However, partial coincidence can occur for certain other rotations about an axis. Two crystal lattices related by such an angular rotation about an axis have certain common sites, located on a single lattice of larger cell dimensions. This larger lattice is called the coincidence site lattice and the boundary it gives rise to is termed a special boundary. Table I gives the axis-angle values which lead to coincidence site lattices. Such special boundaries can minimize their energy by following planes of dense coincidence. (Table II.) A grain boundary running at a small angle to this plane will take up a stepped structure such that it has a maximum surface area in the close-packed planes of the coincidence site lattice, analogous to a dislocation constrained to be along a direction that is not a low energy direction. This step structure is shown in Fig. 7 at BC. This figure is a two-dimensional model for a b.c.c. bicrystal with a coincidence site density of 1 in 11. The model thus gives a satisfactory explanation for the origin of ledges of the type postulated by McLean.[13]

It is obvious that perfect coincidence is destroyed even with the least deviation of axis or angle from that required for a special relationship to exist between the two crystals. Field ion micrographs of

grain boundaries which do not possess coincidence site relationships also show fit and misfit regions. This can only be explained if the coincidence model can retain some significance even for general high angle boundaries. It is also known from the work of Aust and Rutter[14] that certain special characteristics of boundaries persist over a small range of misorientations around that of the special boundary.

All the above observations can be explained if the random boundary is considered to be composed of a special boundary and an associated sub-boundary to account for the angular (or axial, these are equivalent) deviation. The situation is analogous to a low-angle boundary on real lattice planes at a rotation of 0°. In the case of the random boundary, the dislocations are partial dislocations in the coincidence lattice. The preservation of the identity of dislocations forming the super-posed sub-boundary requires that only small angular deviations of about 6° from the orientation relationship characteristic of a special boundary can be explained in this manner. It is seen from Table I that special boundaries upto a significant coincidence and an angular spread of 6° offer reasonable coverage of the orientations.

The random boundary thus differs from the special boundary not so much in the absence of atoms common to both grains (as would be expected from a rigid model) but in the presence of excess dislocations forming a super-imposed sub-boundary network. Because coincidence regions still occur within the cells of the network the Mott model of the boundary is still a good one, and if the dislocations are sufficiently widely spaced, a ledge structure, as deduced for the general case of a coincidence boundary will still exist.

6.2 Observations

The model advanced by Brandon et al.[11] demands a structure based on dislocations for most orientations. The evidence for the dislocations rested on dark bands observed at random boundaries. Figure 8 shows a bicrystal. The axis of the misorientation is [110] and the angle of misorientation across the boundary is 62°. The nearest coincidence site relationship is for a misorientation of 59° corresponding to a density of coincidence of 1 in 33. Thus this boundary could be described as a low density coincidence boundary together with a dislocation network at the boundary. The dark band is similar to those that had been observed earlier at low angle boundaries by Brandon and his coworkers[15] and had been attributed earlier to the effect of preferential evaporation occurring as a result of the strain field of the dislocations. Further observations[16] have shown that this effect does not occur at all low angle boundaries. It appears that electronic effects can play an important part in the image contrast at grain boundaries and can lead to the appearance of streaks and dark bands. This has been discussed by Ranganathan et al.[17] In this section direct evidence for the presence of dislocations at grain boundaries will be given and then analyzed.

Figure 9 is a micrograph from a tungsten specimen containing a 50° tilt boundary. The axis of misorientation is [110] and the plane of the boundary is (332). An accurate determination of the orientation relationships was possible in this case as the tip was symmetrical and [110] was at the center of the micrograph. The relationship corresponds to a lattice coincidence between the two grains with a density of coincidence sites of 1 in 11. The two-dimensional coincidence site model given in Fig. 7 corresponds to the same rotation about the same axis. The boundary lies

very nearly along the most densely packed plane in the coincidence site lattice, where all the atoms are located on coincidence sites. There are a few ledges of ~10Å dimensions to be seen in Fig. 9. The atomic fit at the boundary is excellent and there is no evidence for preferential evaporation.

Figure 10 shows a grain boundary in molybdenum. The misorientation is around the [110] axis and is 30°. The relationship is 3° away from [110] - 27° which represents a special boundary with a density of coincidence of 1 in 19. One can then consider the boundary to be made up of this special boundary and a 3° small angle boundary. The spiral effect seen in the (110) planes has its origin in the latter boundary. The boundary plane is a few degrees off $(1\bar{1}0)_B$ and $(3\bar{3}2)_A$ and is near a densely packed coincidence site lattice plane of [331] type in both crystals. This accounts for the atomic matching across the boundary.

In the iridium example the dislocation formed part of a low angle boundary: in the case of tungsten, it accounted for the deviation of the grain boundary from a close-packed plane. Now in molybdenum a similar spiral forms part of the small angle boundary superposed on a special boundary.

Figure 11 shows a tricrystal in iridium. The boundary B-C corresponds to a 6° misorientation around [111]. The boundary appears very nearly as a streak. Most (111) planes are seen to join smoothly across the boundary. Boundary A-B is a high angle boundary with a misorientation of 52° around [111]. The nearest coincidence site lattice is 5° away. The boundary is quite narrow and showed extremely good fit over nearly a hundred layers. The good fit observed at the boundary A-B merits some discussion. The orientation relationship for this boundary is 5° away from [111] - 47°

which is the relationship for a coincidence site lattice of $\Sigma = 19$. This lattice is illustrated in Fig. 12. It can be seen that the density of coincidence is so low in this case that an associated 5° sub-boundary will take out almost all lattice coincidence.

Figure 13 shows a [110] - 28° boundary in tungsten. There appears to be a dark band associated with the boundary. On field evaporation this band became less prominent as the intersection of the boundary moved inwards due to the inclination of the plane of the boundary to the axes of the tip. One can see a series of interlocked spirals. In some regions the continuation of the (110) planes across the boundary can be followed through a number of planes.

6.3 Discussion

Field ion micrographs of high angle grain boundaries show three types of structures. In one kind, the planes continue undisturbed across the boundary. Such structures have been observed in twins[4,7] as well as a 110-32° boundary in tungsten.[10] It is possible however that these boundaries can contain dislocations which have their Burgers vector parallel to the undisturbed planes. In the second kind spiral structures which can generally be associated with dislocations have been observed. Most boundaries generally show a greater degree of disturbance at the boundary. Even in such cases the boundary shows good fit over a few regions. The conclusions to be drawn are that all the observations support the transition lattice theory which states that the disturbance is confined to a few atom diameters near the boundary and that the two lattices continue right up to the boundary.[5] It can further be inferred that the boundaries consist of regions of fit and misfit. Mott[18] originally proposed such a

model. The coincidence site lattice model of Brandon et al[11] is an attempt to characterise the regions of fit and misfit in crystallographic terms. Section 6.2 gave the evidence available for such a model from field ion micrographs. (Brandon[19] has recently extended the theoretical part of the model in a rigorous way.)

7. PROPERTIES OF GRAIN BOUNDARIES

Every field ion micrograph of a bicrystal can in principle be used to draw some information concerning atomic configuration at grain boundaries. That it also contains interesting details about the properties of grain boundaries is often a matter of chance. The small field of view and the loss in image intensity and resolution at high temperatures act as severe limitations.

Both thermally activated and stress induced migration of grain boundaries have been observed by the author.[20] It is however difficult to throw any light on the atomistics of the process as the image disappears at high temperatures and as the stress induced migration occurs in an unpredictable manner.

Segregation of oxide at the boundary has been observed in boundaries in tungsten - 5% rhenium.[11] Large bright spots are occasionally observed at boundaries. Their chemical identity is unknown. Investigation of segregation and depletion near grain boundaries is a fruitful field where very little has been done until now.

Grain boundaries in general increase the strength of a material as they prevent the easy passage of dislocations. Pile-up of dislocations has been shown to occur at grain boundaries. Li[21] has postulated that under the influence of stress, ledges in grain boundaries can be made to

emit dislocations. Müller[22] has shown that grain boundaries in rhenium hardened the material sufficiently to prevent slip under imaging conditions. Ranganathan and Cottrell[16] have reported a particularly interesting interaction between a dislocation and a grain boundary in iridium.

A number of field ion microscope studies are now directed towards a study of thin film formation through evaporation of metals. These could be modified so that in a bicrystal diffusion along a grain boudary can be investigated.

The field ion microscope lends itself readily to the study of small scale effects arising from radiation damage. Grain boundaries interact with such imperfections in a marked way. The elegant studies of Barnes et al[23] have shown that the ability of grain boundaries to act as sinks and sources for vacancies is important. Bowkett et al[24] have observed a large vacancy cluster ~ 15Å away from a grain boundary in neutron irradiated tungsten. The author[20] has carried out a preliminary study of helium bubble formation in tungsten and has observed an "incipient" bubble near a low angle grain boundary.

One fruitful line of investigation would have been the study of specificity of adsorption at grain boundaries. Ehrlich and Hudda[25] have shown that adsorbed atoms can be imaged with the field ion microscope. Brenner[26] carried out experiments to determine whether there is enhanced binding of adsorbed gas atoms at grain boundaries. He found that adsorption seemed to occur preferentially at the edge of the (110) planes but not at the boundary.

8. INTERPHASE INTERFACES

The atomic configuration of an interface separating two crystals which differ in composition and structure presents problems similar to

that of the atomic configuration at high angle grain boundaries. However very few studies have been carried out. Ralph and Brandon[3] have observed that a σ-phase precipitate particle in the 34% rhenium alloy gave enhanced contrast and that in spite of the lack of crystalline regularity in the disordered matrix, the partial coherency with the matrix was readily detectable. The precipitate did not show many developed crystal planes. Recently McLane and Müller have observed the NiBe- Nickel solid solution interface. The precipitate has a CsCl structure while the matrix (98 at % Ni - 2 at % Be) has a face-centred cubic structure. They also showed a second type of interface across which complete coherence was observed. They tentatively interpreted it as a Guinier-Preston zone. Müller et al[28] have also reported the observation of a lens-shaped martensite plate in a high-carbon steel. While the identification is only tentative, these examples show that much of the promise of the technique is turning into reality.

8. ACKNOWLEDGMENTS

Much of the work reported here formed part of the author's doctorate thesis. The author is grateful to U. K. A. E. A. for the provision of research facilities. It is a pleasure to thank Professor A. H. Cottrell, Dr. D. G. Brandon and other members of the field ion group in Cambridge for many stimulating discussions. The author is also grateful to Professor G. Thomas for encouragement and the United States Atomic Energy Commission for financial support.

TABLE I

Axis-Angle Pair and Corresponding Coincidence in the Cubic System

Axis of rotation	Multiplicity	Least angle of rotation	Axis of rotation	Multiplicity	Least angle of rotation
A	Σ	ω	A	Σ	ω
100	5	36.9°	310	5	180°
100	13a	22.6°	310	7	115.4°
100	17a	28.1°	310	11	141.9°
110	3	70.5°	310	13b	76.7°
110	9	38.9°	310	19a	93°
110	11	50.5°	311	3	146.4°
110	17b	86.6°	311	5	95.7°
110	19a	26.5°	311	9	67.1°
111	3	60°	311	11	180°
111	7	38.2°	311	15	50.7°
111	13b	27.8°	311	15	117.9°
111	19b	46.8°	320	7	149°
210	3	131.8°	320	11	100.5°
210	5	180°	320	13a	180°
210	7	73.4°	320	17b	121.9°
210	9	96.4°	320	19b	71.6°
210	15	48.2°	321	7	180°
211	3	180°	321	9	123.7°
211	5	101.6°	321	15	150.1°
211	7	135.6°	321	15	86.2°
211	11	63°	322	9	152.7°
211	15	78.5°	322	13a	107.9°
221	5	143.1°	322	17b	180°
221	9	90°	410	9	152.7°
221	9	180°	410	13b	107.9°
221	13b	112.6°	410	17a	180°
221	17b	61.9°			

TABLE I (cont.)

Axis of rotation	Multiplicity	Least angle of rotation
A	Σ	ω
411	9	180°
411	11	129.6°
411	17a	93.4°
411	19b	153.5°
331	5	154.2°
331	7	110.9°
331	11	82.1°
331	17b	63.8°
331	19a	180°

Σs 13, 17 and 19 each generates two systems and these are distinguished by the subscripts 'a' and 'b'.

TABLE II.

Densely Packed Plane in the Coincidence Site Lattice

Σ	Twin System	Densely Packed Plane B. C. C.	F. C. C.
3	111, 112	112	111
5	012, 013	013	012
7	123	123	123
9	122, 114	114	122
11	113, 233	332	113
13a	320, 015	015	320
13b	134	134	134
15	125	125	125
17a	140, 350	350	140
17b	223, 334	334	223
19a	133, 116	116	133
19b	235	235	235

REFERENCES

1. E. G. Brock, J. Appl. Phys., 28, 241 (1957).

2. P. Wolf, 6th Field Emission Symposium, Washington, D. C., 1959.

3. B. Ralph and D. G. Brandon, Phil. Mag., 8, 919 (1963).

4. J. Hren, Acta Met., 13, 479 (1965).

5. S. Amelinckx and W. Dekeyser, Solid State Physics, 8, 325 (1959).

6. E. W. Müller, Acta Met., 6, 620 (1958).

7. E. W. Müller and O. Nishikawa, Technical Report AFML-TR-65-201, August 1965.

8. E. O. Hall, Twinning (Butterworths Scientific Publications, London, 1954).

9. E. Votava and A. Berghezan, Acta Met., 7, 392 (1959).

10. H. F. Ryan and J. Suiter, Acta Met., (in press).

11. D. G. Brandon, B. Ralph, S. Ranganathan and M. Wald, Acta Met., 12, 813 (1964).

12. S. Ranganathan, Acta Cryst., (in press).

13. D. McLean, J. Aust. Inst. Metals, 8, 45 (1963).

14. K. T. Aust and J. W. Rutter, Recovery and Recrystallization of Metals, L. Himmel, Editor (Interscience Publishers, New York, 1963).

15. D. G. Brandon, M. Wald, M. J. Southon and B. Ralph, J. Phys. Soc., Japan, 18, 324 (1963).

16. S. Ranganathan and A. H. Cottrell, Electron Microscopy, Prague, 1964, p. 163.

17. S. Ranganathan, K. M. Bowkett, J. Hren and B. Ralph, Phil. Mag., 12, 841 (1965).

18. N. F. Mott, Proc. Phys. Soc., 60, 391 (1948).

19. D. G. Brandon, Acta Met., (submitted for publication).

20. S. Ranganathan, (Ph. D. Thesis), Cambridge University, 1965.

21. J. C. M. Li, J. Aust. Inst. Metals, 8, 206 (1963).

22. E. W. Müller, Electron Microscopy 1964, Prague, 1964, p. 161.

23. R. S. Barnes, G. B. Redding and A. H. Cottrell, Phil. Mag., 3, 97 (1958).

24. K. M. Bowkett, J. Hren and B. Ralph, Electron Microscopy 1964, Prague 1964, p. 191.

25. G. Ehrlich and F. G. Hudda, J. Chem. Phys., 36, 3233 (1962).

26. S. S. Brenner, ASM Publication on Metal Surfaces, 1962.

27. S. B. McLane and E. W. Müller, 12th Field Emission Symposium, University Park, Pennsylvania.

28. E. W. Müller, S. Nakamura, O. Nishikawa, and S. B. McLane, J. Appl. Phys., 36, 2496 (1965).

FIGURE CAPTIONS

Fig. 1a Determination of angle and axis of misorientation from the stereographic projection of a bicrystal. (P = pole; M = mid-point of arc joining corresponding poles).

Fig. 1b Determination of the orientation of the plane of the boundary.

Fig. 1c The three types of orientation of the boundary plane and their appearance on a stereographic projection.

Fig. 2 A low angle boundary with a misorientation of 2° around [111] in iridium.

Fig. 3 A noncoherent twin boundary in tungsten.

Fig. 4 Image from a tungsten tip before deformation twinning in situ occurred.

Fig. 5 Same as Fig. 4 after deformation twinning.

Fig. 6 A deformation twin interface in tungsten.

Fig. 7 Two dimensional model for a b.c.c. bicrystal with a coincidence site density of 1 in 11.

Fig. 8 A bicrystal in tungsten. The boundary appears as a dark band.

Fig. 9 A special boundary in tungsten with a coincidence site density of 1 in 11.

Fig. 10 A random boundary in molybdenum. The boundary is composed of a special boundary and a small angle boundary. The spiral effect has its origin in the latter effect.

Fig. 11 Tri-crystal in iridium.

Fig. 12 Coincidence site model for the high angle boundary in the tri-crystal in Fig. 11.

Fig. 13 [110] - 28° boundary in tungsten. The deviation from lattice coincidence is slight in this case.

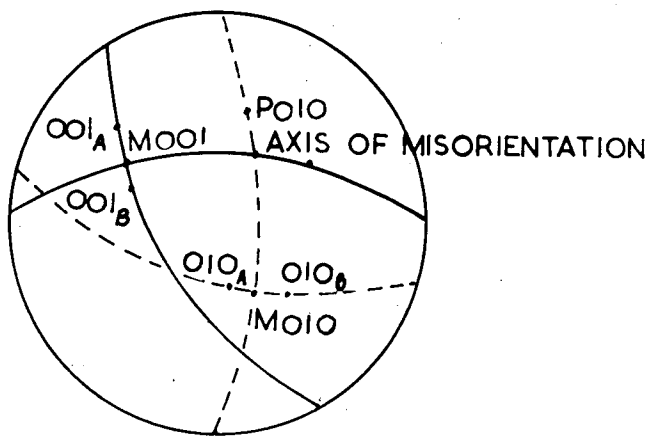

a

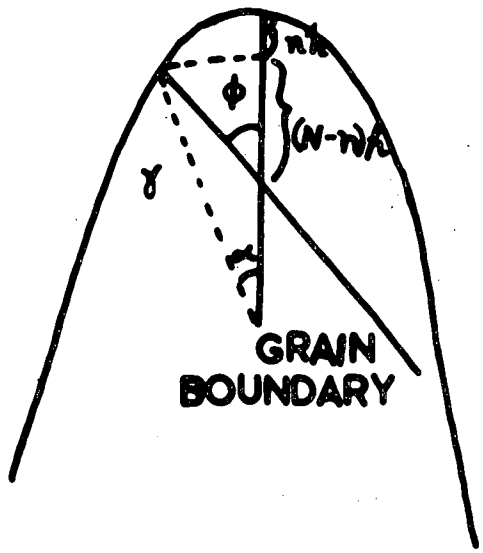

b

MUB-10098

Fig. 1a, b

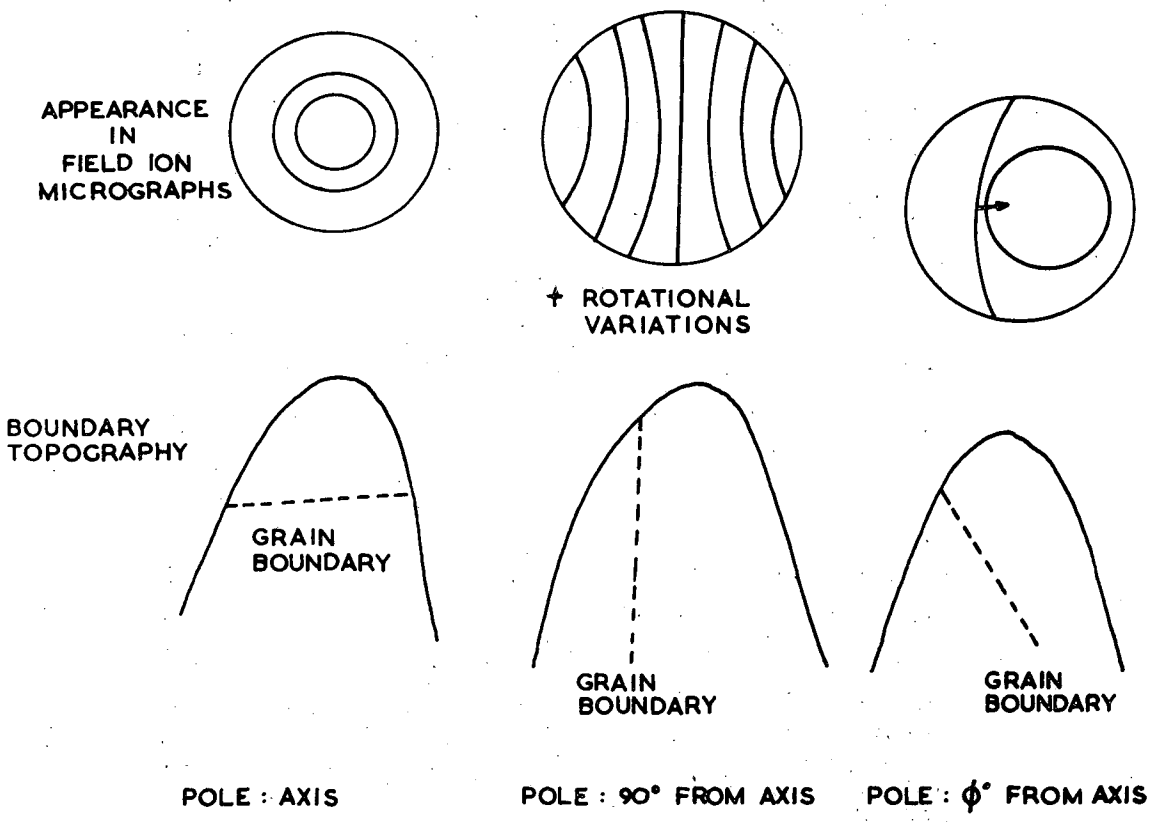

C

MUB-10099

Fig. 1c

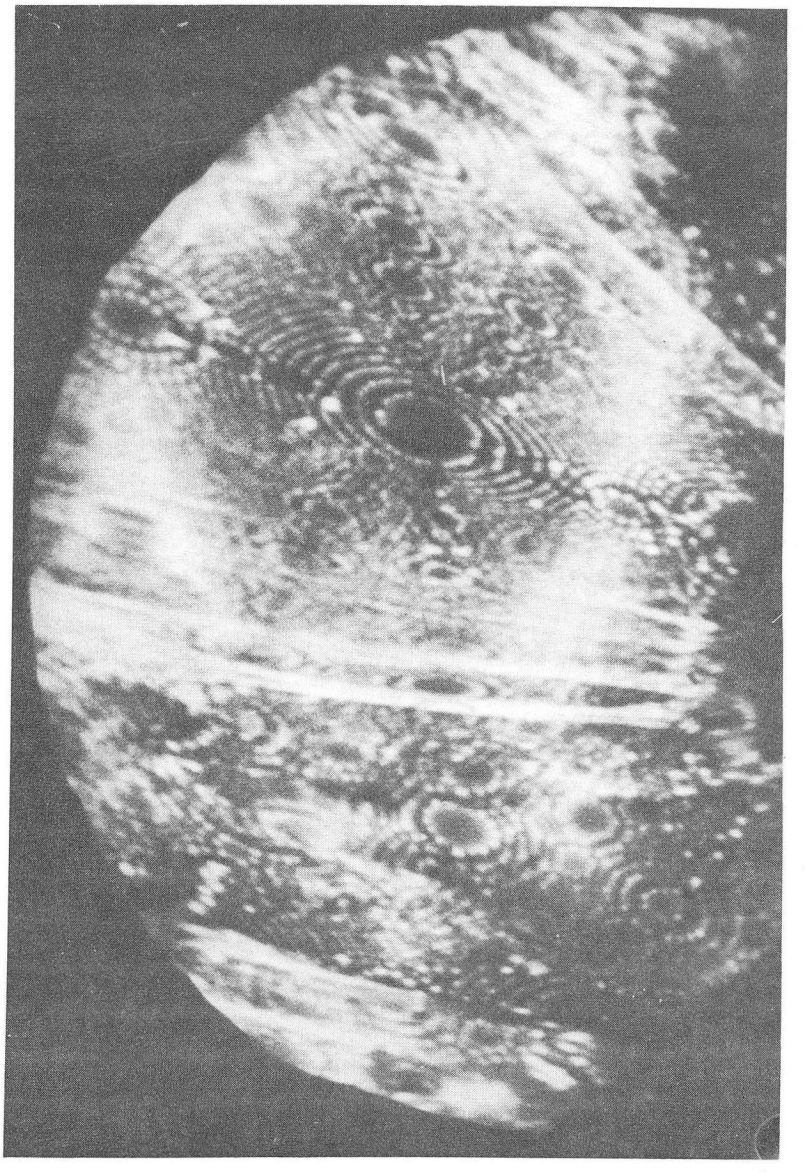

ZN-5393

Fig. 2

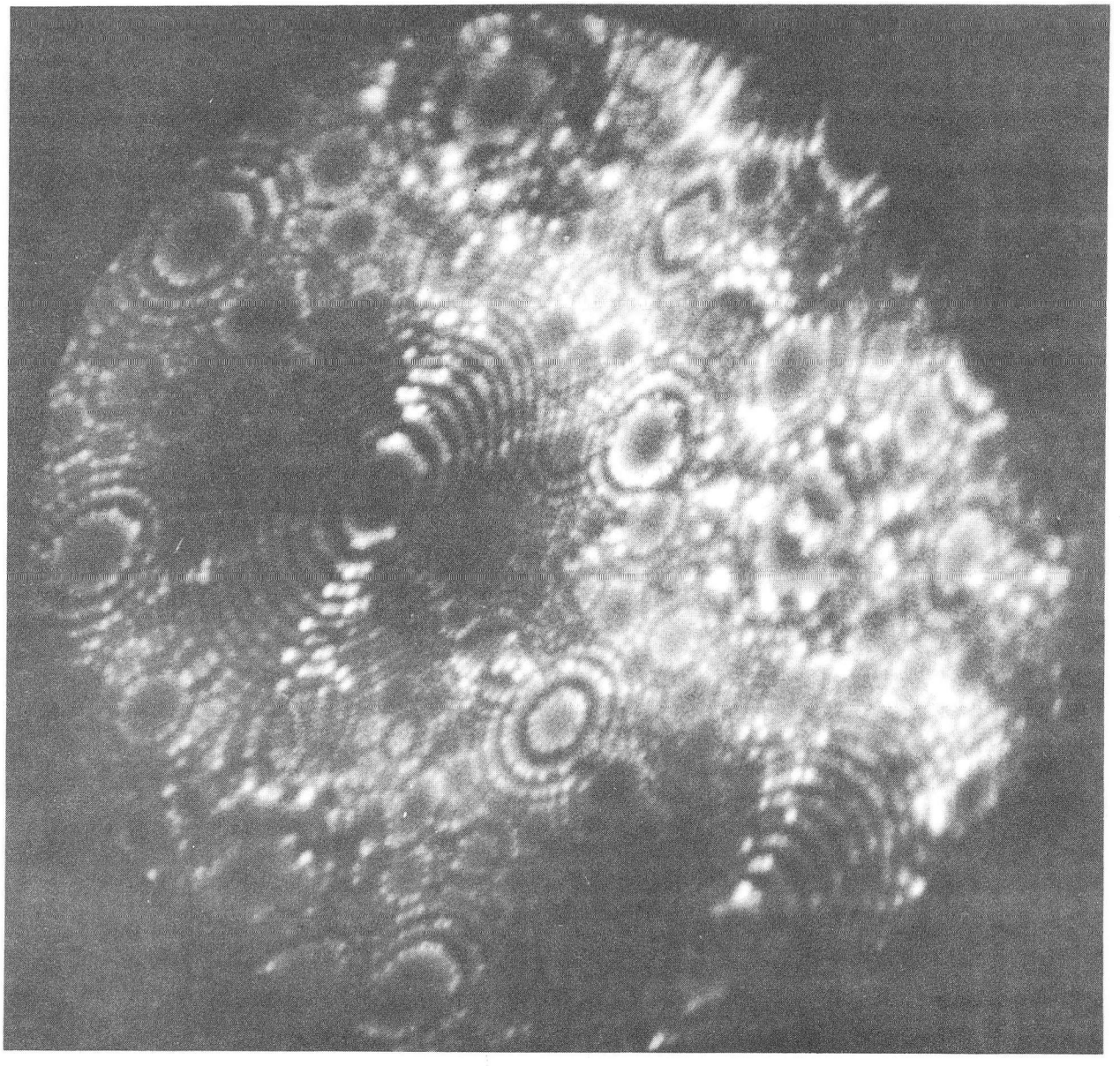

ZN-5451

Fig 3a-

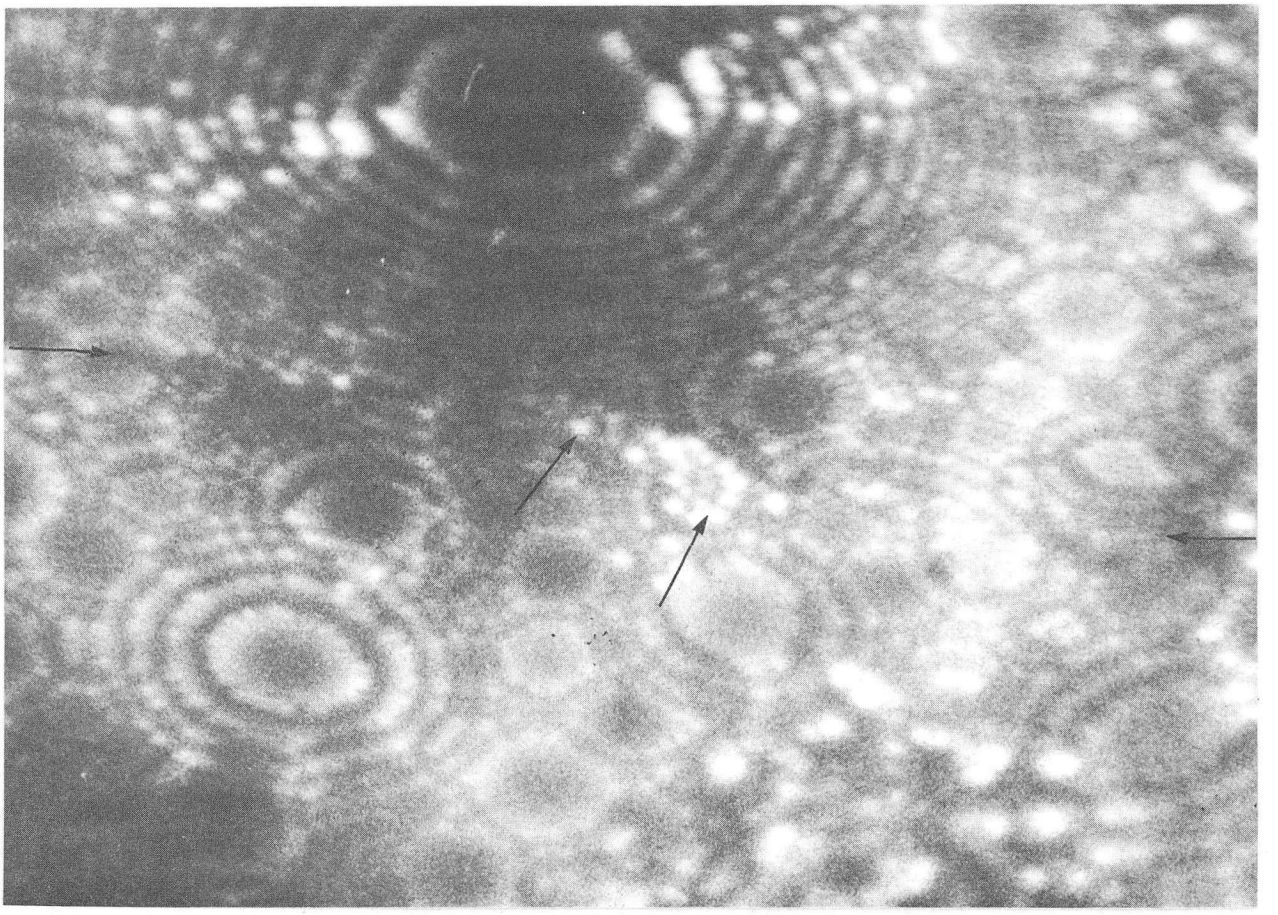

ZN-5455

Fig. 3b-

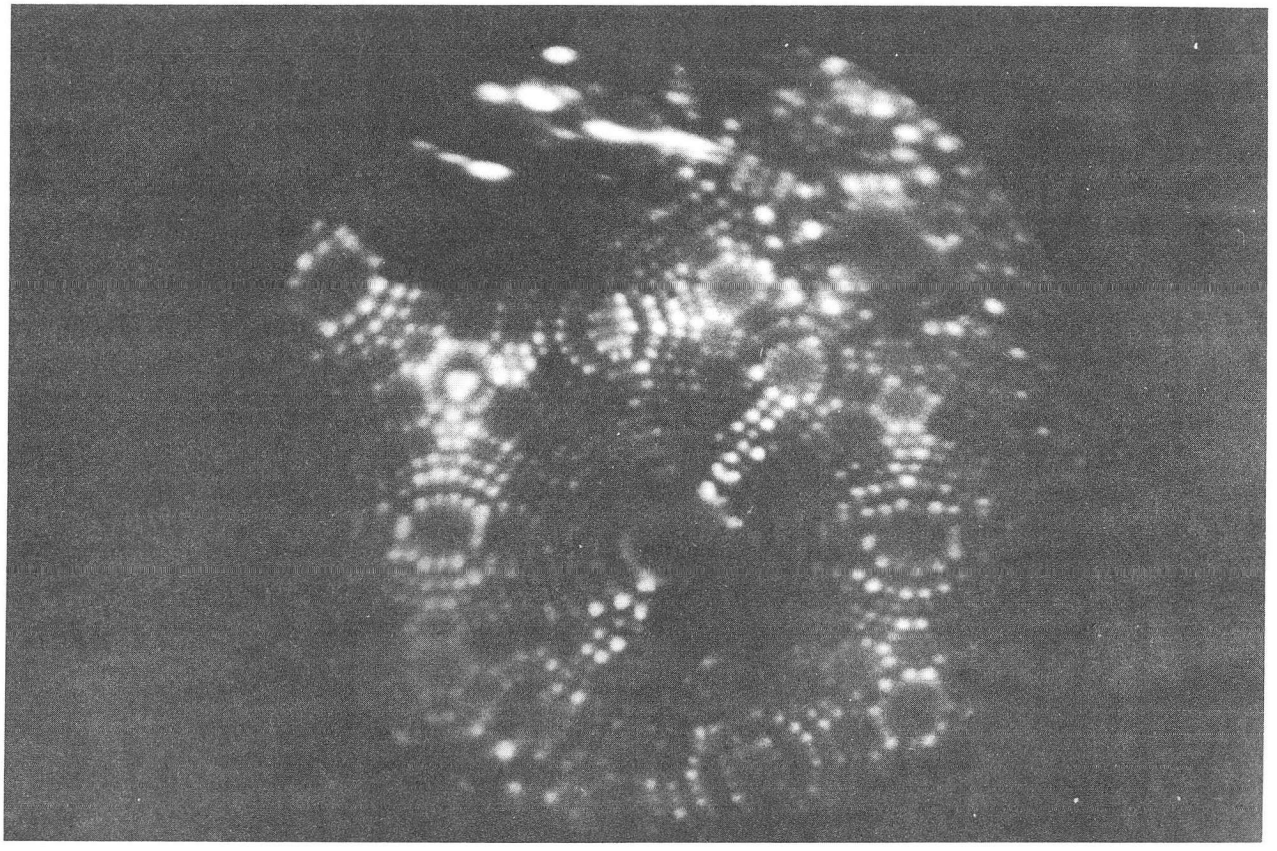

ZN-5454

Fig. 4

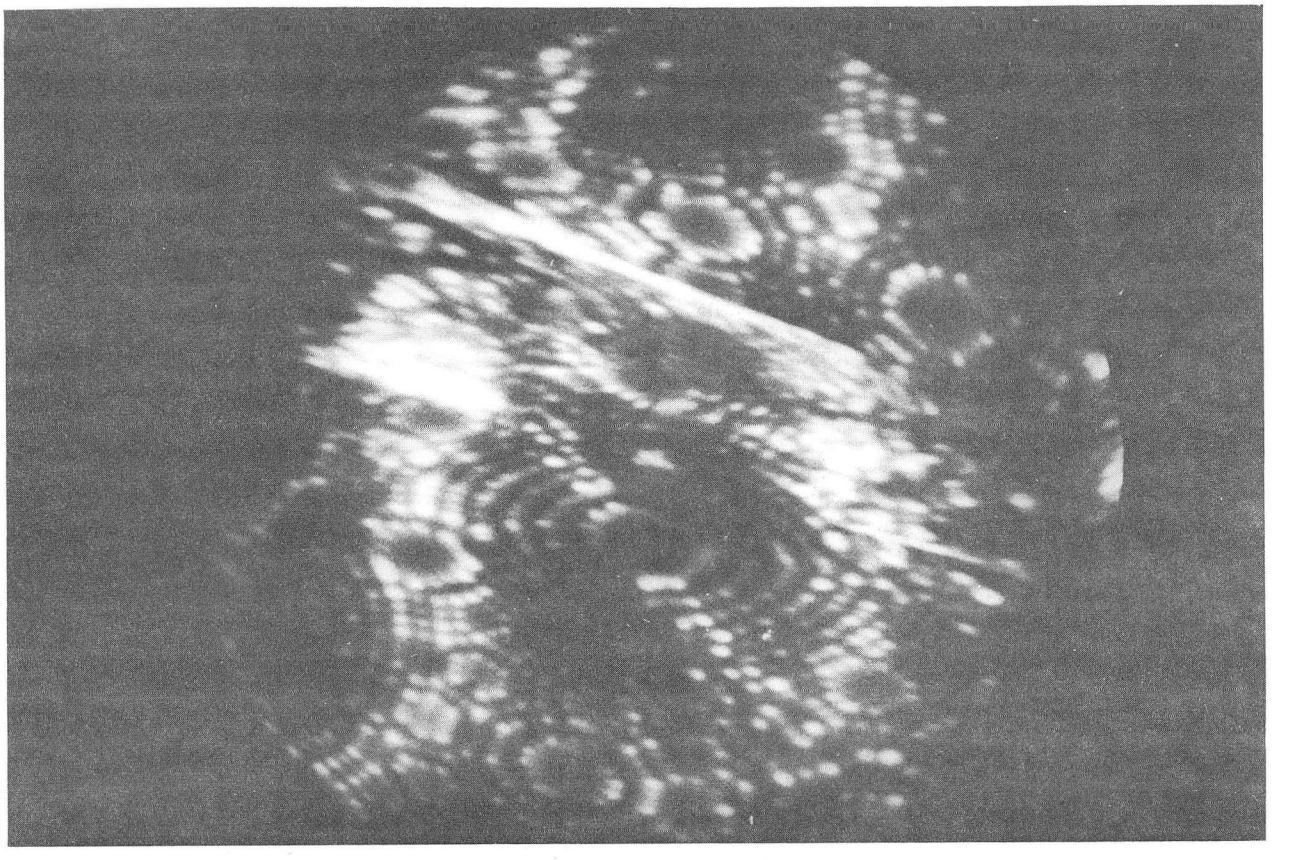

ZN-5450

Fig. 5

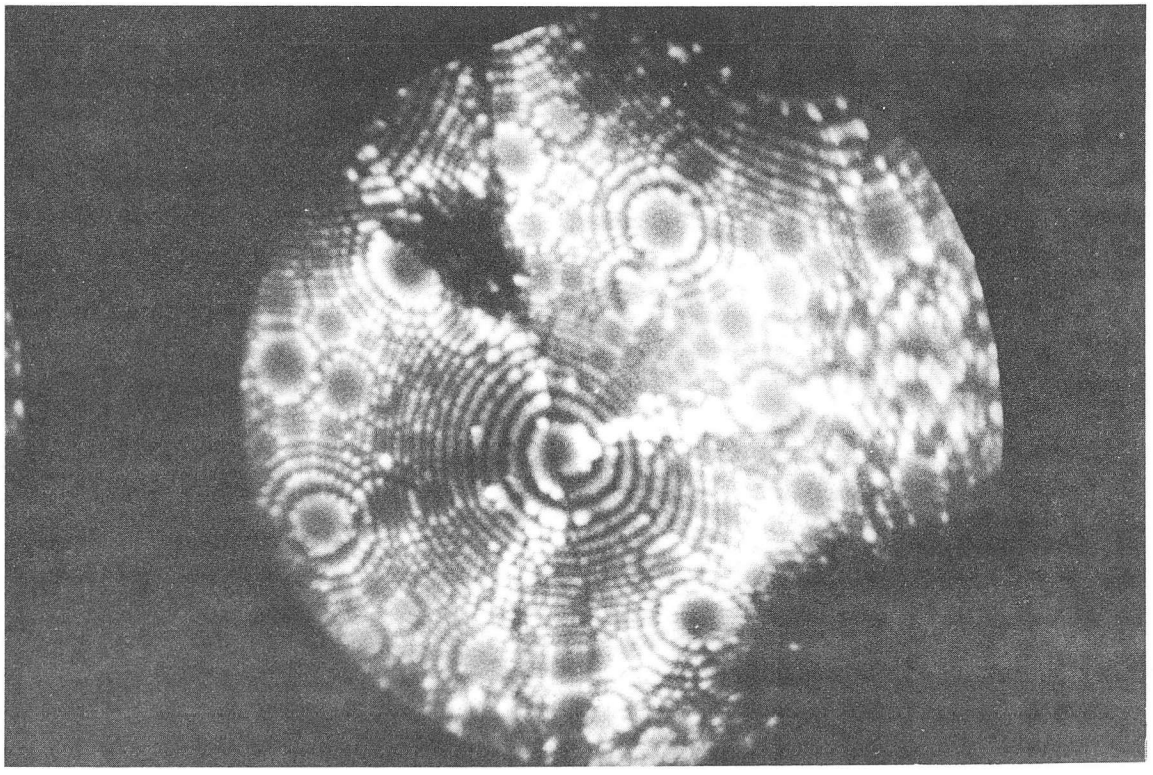

ZN-5290

Fig. 6

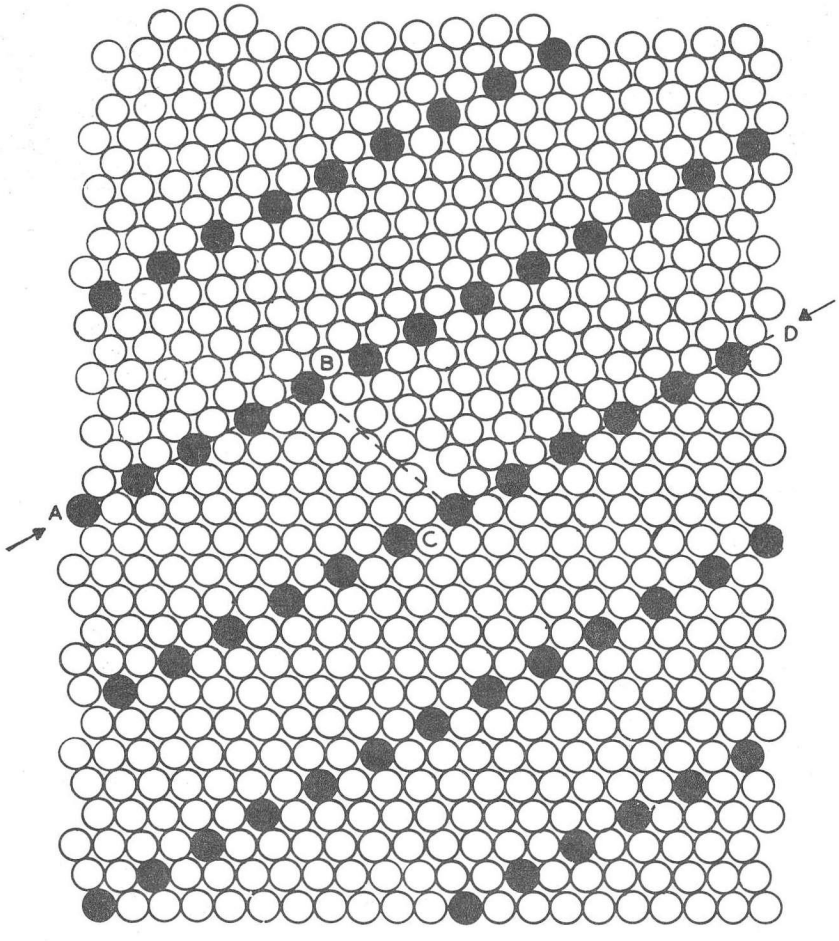

Fig. 7

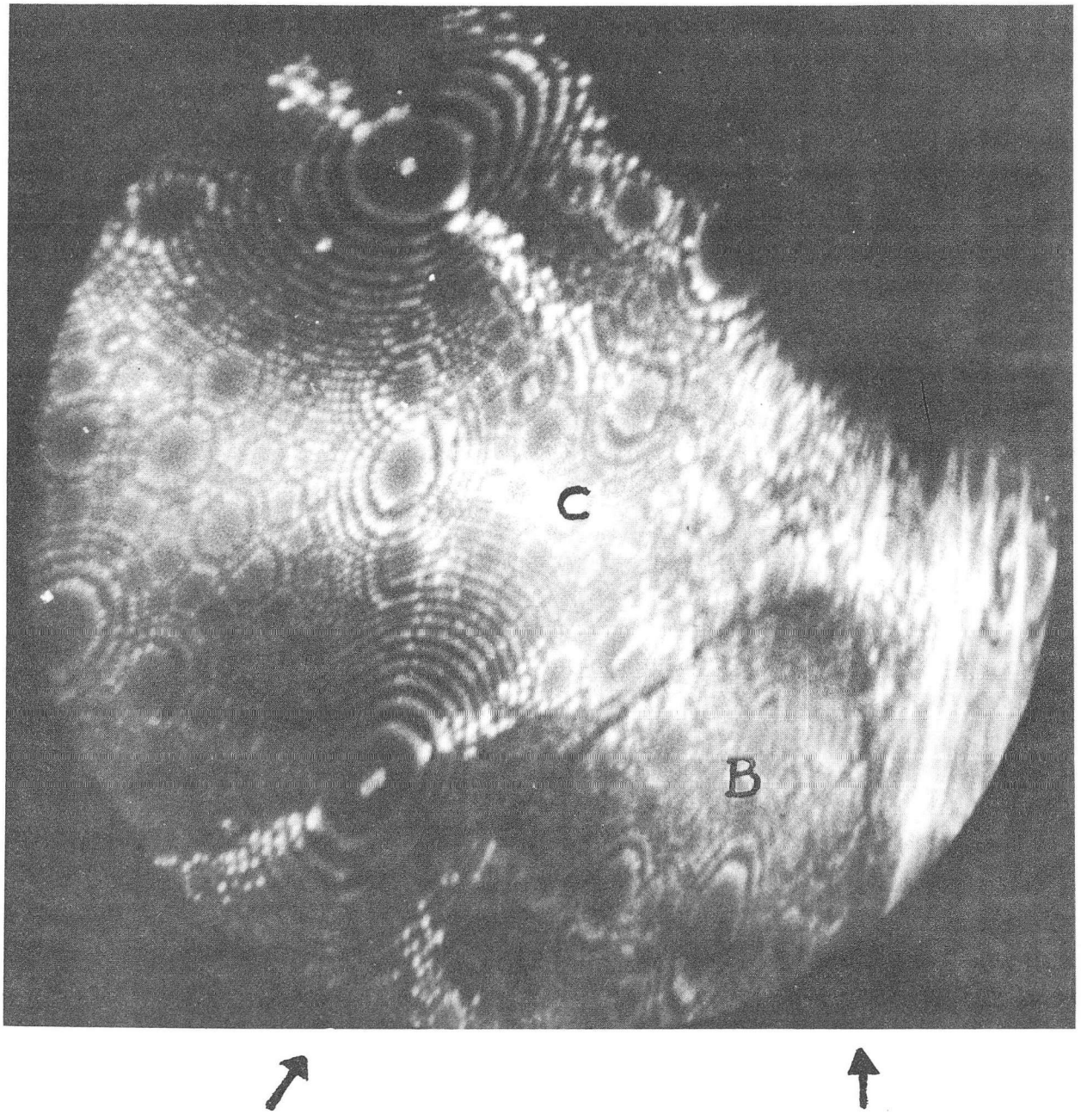

ZN-5456

Fig. 8

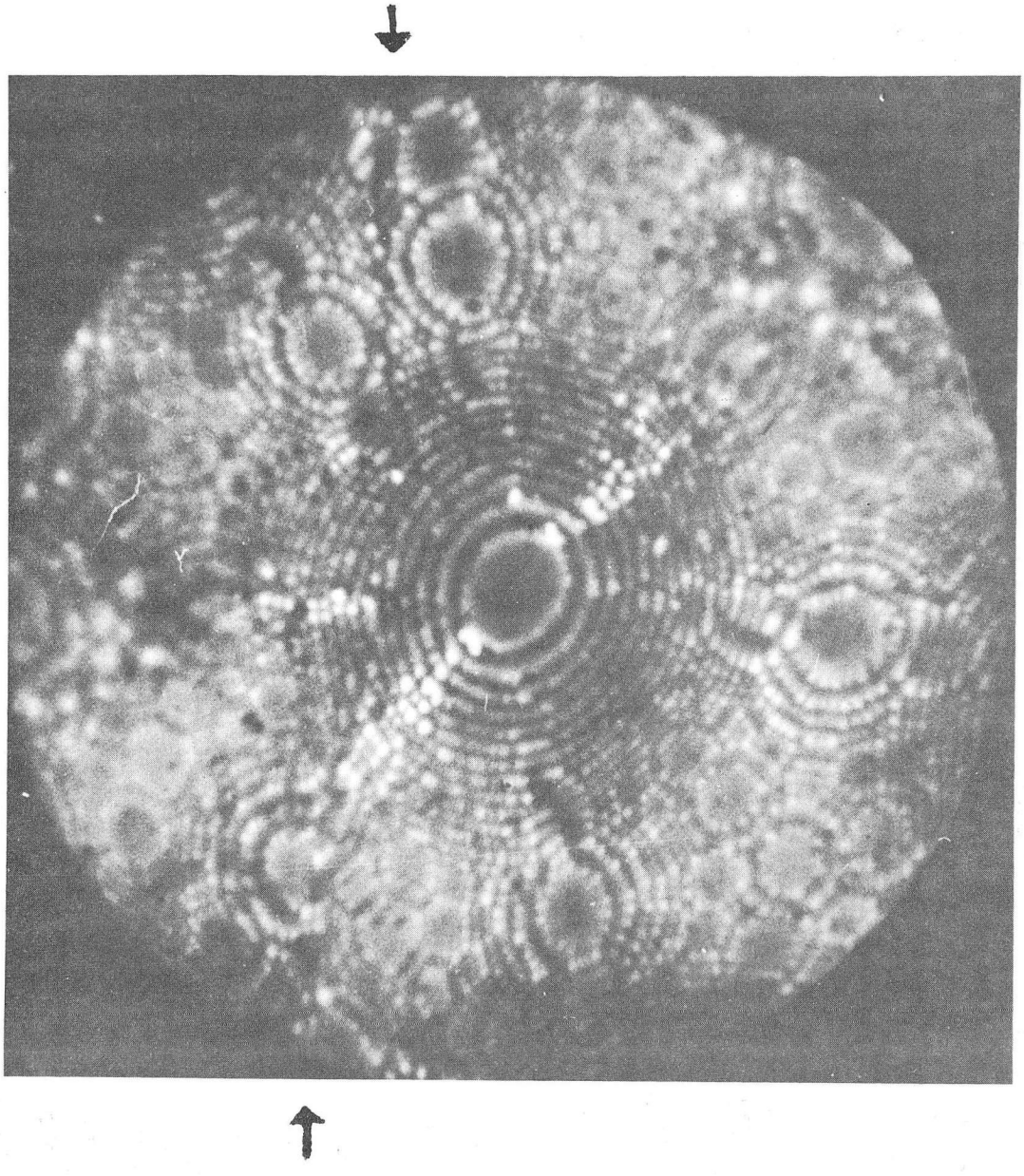

ZN-5457

Fig. 9

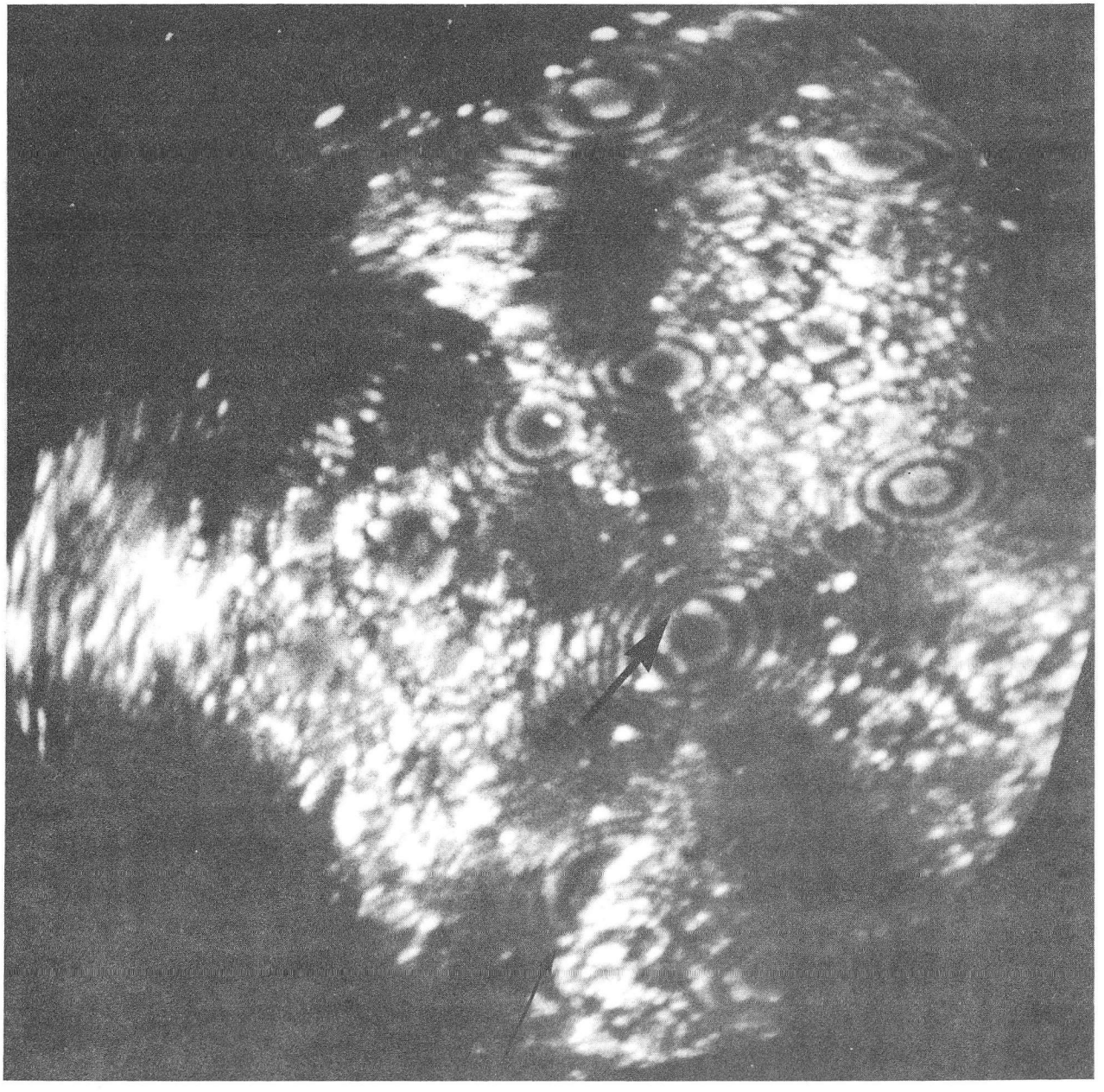

ZN-5452

Fig. 10

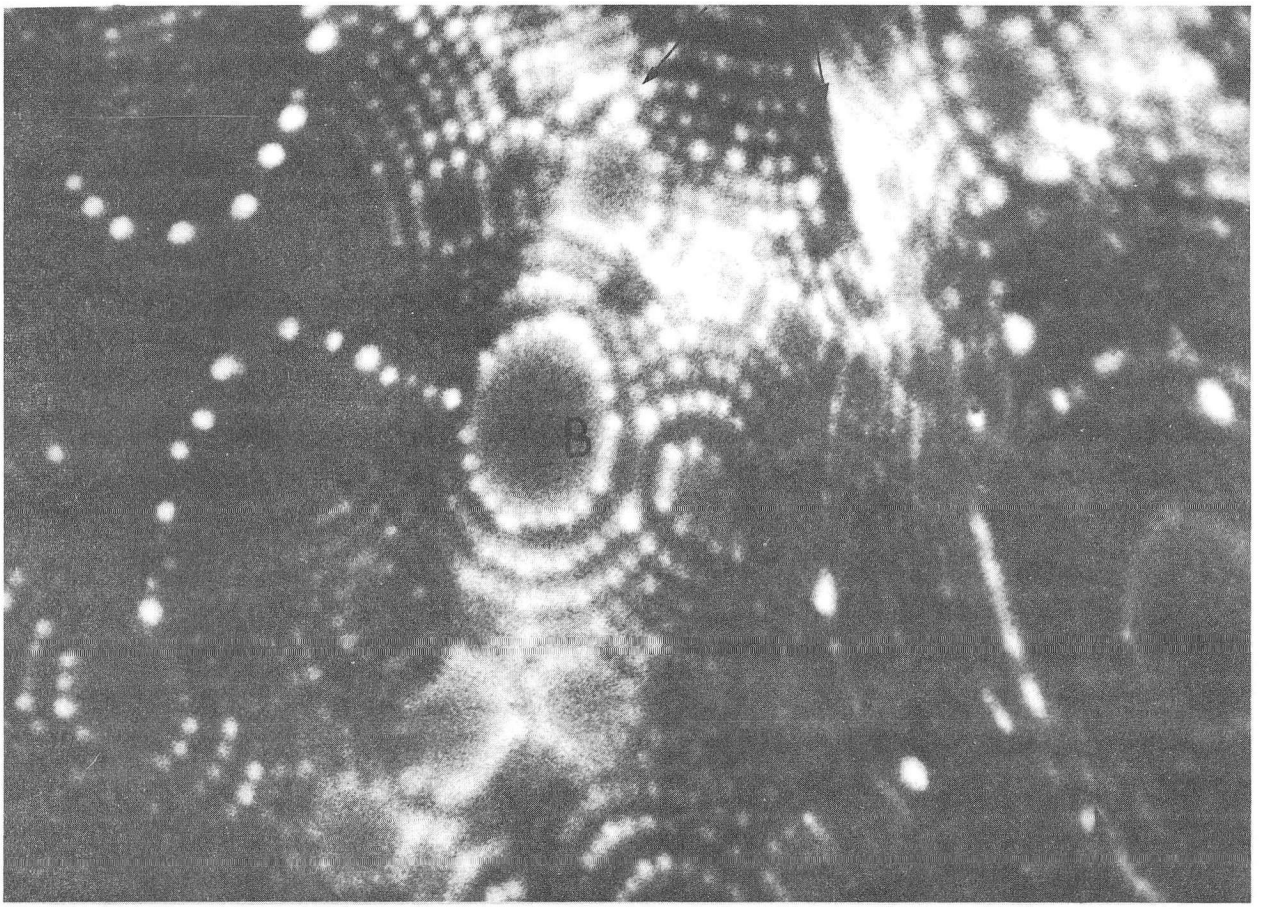

ZN-5453

Fig. 11

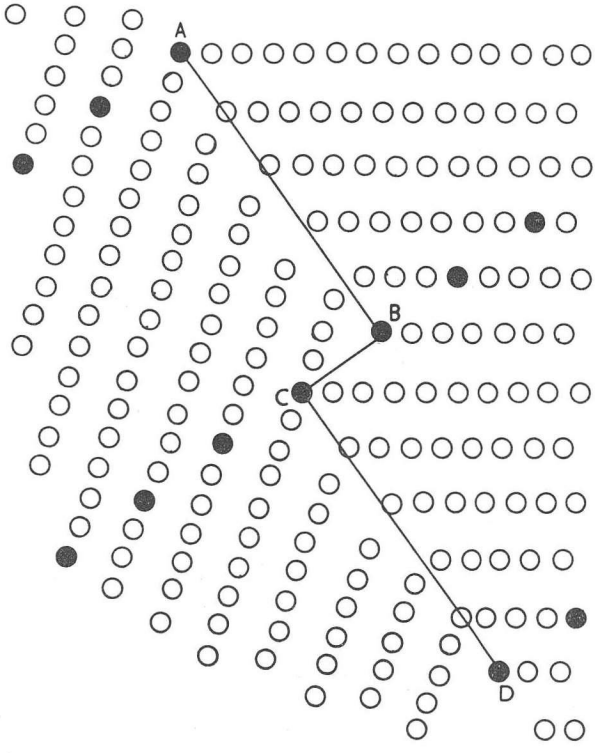

MUB-10097

Fig. 12

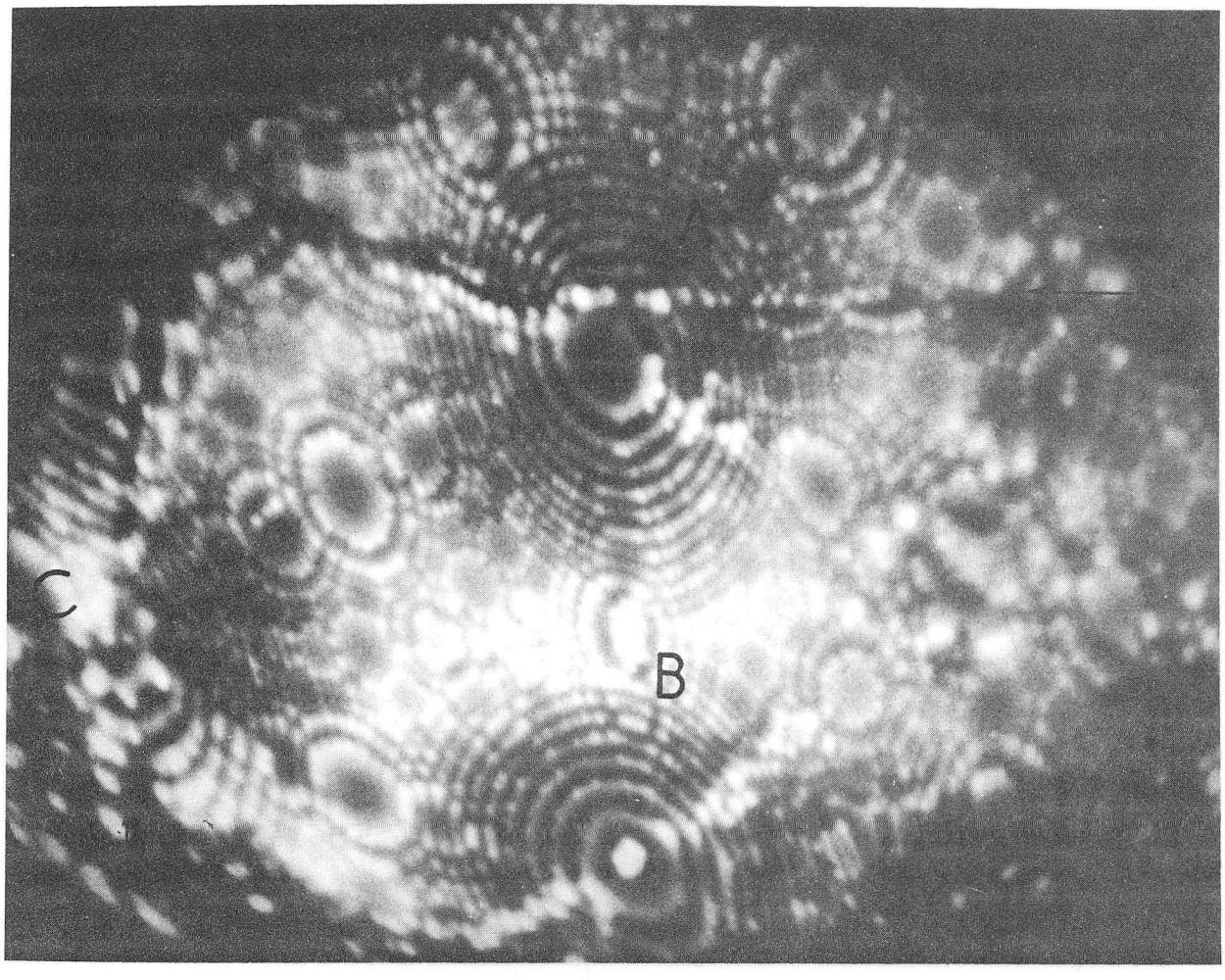

ZN-5458

Fig. 13

This report was prepared as an account of Government sponsored work. Neither the United States, nor the Commission, nor any person acting on behalf of the Commission:

A. Makes any warranty or representation, expressed or implied, with respect to the accuracy, completeness, or usefulness of the information contained in this report, or that the use of any information, apparatus, method, or process disclosed in this report may not infringe privately owned rights; or

B. Assumes any liabilities with respect to the use of, or for damages resulting from the use of any information, apparatus, method, or process disclosed in this report.

As used in the above, "person acting on behalf of the Commission" includes any employee or contractor of the Commission, or employee of such contractor, to the extent that such employee or contractor of the Commission, or employee of such contractor prepares, disseminates, or provides access to, any information pursuant to his employment or contract with the Commission, or his employment with such contractor.